

Band offsets and electronic properties of the Ga_2O_3/FTO heterojunction via transfer of free-standing Ga_2O_3 onto FTO/glass

Xia Wang(王霞), Wei-Fang Gu(古卫芳), Yong-Feng Qiao(乔永凤), Zhi-Yong Feng(冯志永), Yue-Hua An(安跃华), Shao-Hui Zhang(张少辉), and Zeng Liu(刘增)

Citation: Chin. Phys. B, 2021, 30 (**11**): 114211. DOI: 10.1088/1674-1056/ac11e7
Journal homepage: http://cpb.iphy.ac.cn; http://iopscience.iop.org/cpb

What follows is a list of articles you may be interested in

Ultrafast carrier dynamics of Cu_2O thin film induced by two-photon excitation

Jian Liu(刘建), Jing Li(李敬), Kai-Jun Mu(牧凯军), Xin-Wei Shi(史新伟), Jun-Qiao Wang(王俊俏), Miao Mao(毛淼), Shu Chen(陈述) , and Er-Jun Liang(梁二军)

Chin. Phys. B, 2021, 30 (**11**): 114205. DOI: 10.1088/1674-1056/ac003c

7.6-W diode-pumped femtosecond Yb: KGW laser

Yan-Fang Cao(曹艳芳), Xiang-Hao Meng(孟祥昊), Jun-Li Wang(王军利), Zhao-Hua Wang(王兆华), Meng-Yao Cheng(程梦尧), Jiang-Feng Zhu(朱江峰), Zhi-Yi Wei(魏志义)

Chin. Phys. B, 2019, 28 (**4**): 044205. DOI: 10.1088/1674-1056/28/4/044205

Two-dimensional materials-decorated microfiber devices for pulse generation and shaping in fiber lasers

Zhi-Chao Luo(罗智超), Meng Liu(刘萌), Ai-Ping Luo(罗爱平), Wen-Cheng Xu(徐文成)

Chin. Phys. B, 2018, 27 (**9**): 094215. DOI: 10.1088/1674-1056/27/9/094215

Sb_2Te_3 mode-locked ultrafast fiber laser at 1.93 μm

Jintao Wang(王金涛), Jinde Yin(尹金德), Tingchao He(贺廷超), Peiguang Yan(闫培光)

Chin. Phys. B, 2018, 27 (**8**): 084214. DOI: 10.1088/1674-1056/27/8/084214

Microstructure and optical properties of nitrogen-doped ZnO film

Zhao Xian-Wei, Gao Xiao-Yong, Chen Xian-Mei, Chen Chao, Zhao Meng-Ke

Chin. Phys. B, 2013, 22 (**2**): 024202. DOI: 10.1088/1674-1056/22/2/024202

Band offsets and electronic properties of the Ga_2O_3/FTO heterojunction via transfer of free-standing Ga_2O_3 onto FTO/glass*

Xia Wang(王霞)[1,†], Wei-Fang Gu(古卫芳)[1], Yong-Feng Qiao(乔永凤)[1], Zhi-Yong Feng(冯志永)[1], Yue-Hua An(安跃华)[2], Shao-Hui Zhang(张少辉)[3], and Zeng Liu(刘增)[4,5]

[1] *Department of Electrical Engineering and Automation, Shanxi Institute of Technology, Yangquan* 045000, *China*
[2] *School of Optoelectronic Engineering, Guangdong Polytechnic Normal University, Guangzhou* 510665, *China*
[3] *Shenzhen Engineering Laboratory of Phosphorene and Optoelectronics, International Collaborative Laboratory of 2D Materials for Optoelectronics Science and Technology of Ministry of Education, College of Optoelectronic Engineering, Shenzhen University, Shenzhen* 518060, *China*
[4] *College of Electronic and Optical Engineering & College of Microelectronics, Nanjing University of Posts and Telecommunications, Nanjing* 210023, *China*
[5] *National and Local Joint Engineering Laboratory for RF Integration and Micro-Packing Technologies, Nanjing University of Posts and Telecommunications, Nanjing* 210023, *China*

(Received 1 June 2021; revised manuscript received 30 June 2021; accepted manuscript online 7 July 2021)

The determination of band offsets is crucial in the optimization of Ga_2O_3-based devices, since the band alignment types could determine the operations of devices due to the restriction of carrier transport across the heterogeneous interfaces. In this work, the band offsets of the Ga_2O_3/FTO heterojunction are studied using x-ray photoelectron spectroscopy (XPS) based on Kraut's method, which suggests a staggered type-II alignment with a conduction band offset (ΔE_C) of 1.66 eV and a valence band offset (ΔE_V) of −2.41 eV. Furthermore, the electronic properties of the Ga_2O_3/FTO heterostructure are also measured, both in the dark and under ultraviolet (UV) illuminated conditions (254 nm UV light). Overall, this work can provide meaningful guidance for the design and construction of oxide hetero-structured devices based on wide-bandgap semiconducting Ga_2O_3.

Keywords: Ga_2O_3/FTO heterojunction, band alignment, magnetron sputtering, free-standing

PACS: 42.70.Nq, 42.70.−a, 85.60.Gz **DOI:** 10.1088/1674-1056/ac11e7

1. Introduction

Oxide semiconductors are always regarded as important materials due to their optical transparency, high mobility and mature preparation technologies, catering for many applications, and have been developed in scientific and technological fields of photonic and optoelectronic devices.[1] In an oxide system, the band alignment of the oxide heterojunction plays a very important role in governing the functional electronic devices, since the device performances are seriously affected by the carrier transport at the heterogeneous interfaces.[2,3]

Over the last two decades, Ga_2O_3, a very important and promising oxide semiconductor material, has become a candidate in the fabrication of solar-blind UV photodetectors, high-power electronics, and radiation-resistant optoelectronics, which are benefited by its ultra-wide bandgap ($E_g \sim 5$ eV) and high breakdown critical electrical field ($E_{br} \sim 8$ MV/cm).[4–6] The band offsets at conduction and valence band edges are very important to guide the design of heterogeneous devices. To date, there are a few studies on the band alignments of Ga_2O_3-based heterojunctions,[7] and they have increased significantly in the last 2–3 years. For instance, Rao *et al.* researched the band offsets of p-type oxide (SnO or NiO)/Ga_2O_3 heterojunctions.[8] Zhi *et al.* studied the band offsets of the In_2O_3/Ga_2O_3 heterointerface.[9] The band alignments of the ZnO/Ga_2O_3 and Ta_2O_5/Ga_2O_3 heterointerface were studied by Liu *et al.*[10] The various alignments lead to different functional operations on the basis of the alignment results. In brief, the fabrication of oxide heterojunctions based on Ga_2O_3 at the interface can provide new possibilities to develop oxide heterostructured (opto)electronics.[3,7,11,12]

F-doped SnO_2 (FTO) has inspired interest for use in transparent conductive electrodes (TCEs), transparent optoelectronic devices and flexible display technologies, due to its low cost and strong stability.[13] In comparison, Sn-doped In_2O_3 (ITO) conducts electricity well;[14] however, the ITO films exhibit brittleness, poor stability at high temperature and high costs due to the presence of indium.[15] Therefore, as a replacement for ITO, FTO has a wide range of applications in constructing electrodes, and sensing and switching devices.[16]

Considering the applications of Ga_2O_3 in flexible and

*Project supported by the Fund of Shanxi Institute of Technology (Grant No. 2021QD-15), 2020 Excellent Doctoral Award Fund for working in Shanxi Province (Shanxi Institute of Technology), China (Grant No. 2021PT-09), and the National Natural Science Foundation of China (Grant No. 62004047).

†Corresponding author. E-mail: tianmingduwu@bupt.cn

© 2021 Chinese Physical Society and IOP Publishing Ltd

transparent optoelectronic devices[17] and the meanings of band alignment for the development of Ga_2O_3 based heterogeneous electronic and optoelectronic devices,[11,18,19] it is necessary to study the band calibration of the Ga_2O_3/FTO heterojunction. The band alignment of the Ga_2O_3/FTO heterojunction can provide a reference for the application of Ga_2O_3/FTO heterojunctions in transparent optoelectronic devices and flexible devices.

In this paper, we construct the Ga_2O_3/FTO heterojunction using radio-frequency (r.f.) magnetron sputtering and free-standing film transfer techniques. Then, the band alignment of the Ga_2O_3/FTO heterojunction is determined using x-ray photoelectron spectroscopy (XPS) and an ultraviolet–visible (UV–Vis) absorbance spectrum. Finally, the electronic properties of the Ga_2O_3/FTO heterojunction are shown and discussed.

2. Experimental details

To obtain the band alignment of the Ga_2O_3/FTO heterojunction, three samples were prepared. The detailed experimental processes are given as follows.

Firstly, three commercially available FTO substrates were cleaned with acetone, ethyl alcohol and deionized water in the appropriate order using an ultrasonic cleaning machine, then dried with a N_2 flow gun.

Secondly, two FTO substrates were used as substrates to deposit Ga_2O_3 by r.f. magnetron sputtering for about 100 min and 1 min, respectively. Thus, three samples, i.e., (i) FTO substrate, (ii) ~ 300 nm Ga_2O_3 on FTO substrate and (iii) < 5 nm Ga_2O_3 on FTO substrate, were finished by fabrication. During deposition, the basic pressure is $\sim 2 \times 10^{-4}$ Pa, and the Ga_2O_3 thin film is deposited at argon pressure of 0.8 Pa and r.f. power of 70 W.

Thirdly, according to Kraut's method,[20,21] the bonding states of Ga_2O_3 and FTO can be determined by XPS scanning data. The charge-shift spectra were calibrated with the adventitious C 1s peak at 284.9 eV. The optical bandgap of FTO was determined by the UV–Vis absorption spectrum and the optical bandgap values of Ga_2O_3 have been reported in our previous works.[22,23]

Finally, the Ga_2O_3/FTO heterojunction on the FTO/glass substrate was fabricated by transferring free-standing Ga_2O_3 film (the detailed experimental descriptions can be seen in Ref. [22]), since high-quality Ga_2O_3 films need to be prepared at 750 °C, which will change the existence of the FTO film (destroy over 550 °C).[23] The current–voltage (I–V) characteristic curves were tested by a Keithley 2450 semiconductor analysis meter. The photocurrent measurement was performed under 254 nm UV light illumination with intensity of 300 μW/cm^2.

3. Results and discussion

Figure 1(a) shows the UV–Vis absorbance spectrum of the FTO thin film and the plot of $[(\alpha hv)^2$ versus $hv]$ is displayed in Fig. 1(a) inset. The bandgap (E_g) of FTO is estimated to be 4.0 eV according to the results in Fig. 1(a) inset, which is comparable to the reported values. The E_g of Ga_2O_3 is about 4.75 eV, which has been described in our previous reports.[22] As the FTO substrate is commercially available, it is necessary to verify the quality of the transferred Ga_2O_3. As shown in Fig. 1(b), the high-resolution transmission electron microscopy (HR-TEM) image suggests that the free-standing Ga_2O_3 film is polycrystalline.[22]

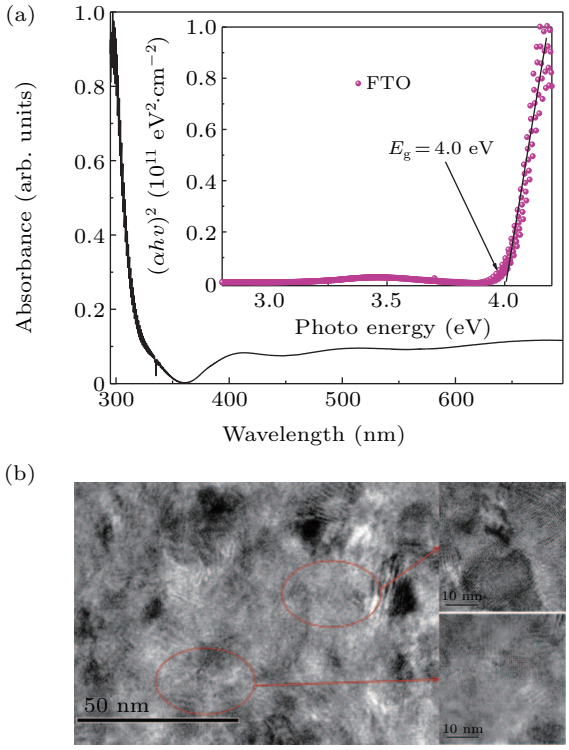


Fig. 1. (a) The UV–Vis absorbance spectrum of FTO; the inset is the plots of $[(\alpha hv)^2$ versus $hv]$, hv is the incident photon energy and α is the absorbance coefficient. (b) The HR-TEM image of the free-standing Ga_2O_3 film.

Figures 2(a) and 2(c) show the valence band minimums (VBMs) for the FTO and Ga_2O_3, respectively. And the high-resolution XPS spectra of the core energy levels for the FTO and Ga_2O_3 are shown in Figs. 2(b) and 2(d), from which we can see that the VBMs of the FTO and Ga_2O_3 are 2.3 eV and 1.9 eV, respectively; the core energy levels of the FTO and Ga_2O_3 are provided with the values of 494.95 eV and 1118.63 eV. Figures 2(e) and 2(f) show the core energy levels of the Ga_2O_3/FTO heterojunction in the XPS spectra. The values of the core energy levels of the Ga_2O_3 and the FTO are 1118.34 eV and 491.85 eV at the Ga_2O_3/FTO heterointerface, respectively. Based on these binding energy values, the ΔE_C and ΔE_V of the Ga_2O_3/FTO (GAO/FTO) heterojunction can be calculated using the following equations.[10,20,21]

Table 1. Values of core energy levels, VBMs and band offsets in this experiment (eV).

Ga_2O_3			FTO			Ga_2O_3 on FTO			
metal core	VBM	core level	metal core	VBM	core level	core (GAO)	core (FTO)	ΔE_V	ΔE_C
Ga $2p_{3/2}$	1.9	1118.63	Sn $3d_{3/2}$	2.3	494.95	1118.34	491.85	−2.41	1.66

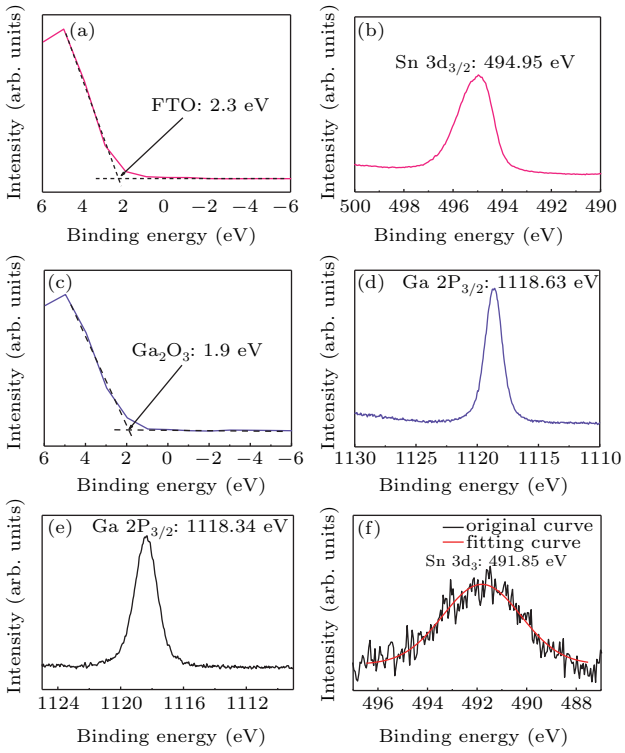


Fig. 2. XPS spectra of (a) VBM of FTO, and (b) the Sn $3d_{3/2}$ core energy level. XPS spectra of (c) VBM of Ga_2O_3, and (d) the Ga $2p_{3/2}$ core energy level. (e) Ga $2p_{3/2}$ core energy levels, and (f) XPS spectra of Sr $3d_{3/2}$ at the $Sr_3Al_2O_6/Ga_2O_3$ interface.

The valence band offset (ΔE_V) is

$$\Delta E_V = (E_{core} - E_{VBM})_{GAO} - (E_{core} - E_{VBM})_{FTO} - (E_{core}^{GAO} - E_{core}^{FTO})_{GAO}^{FTO}, \quad (1)$$

i.e.,

$$\begin{aligned}\Delta E_V &= (1118.63 - 1.9) - (494.95 - 2.3) \\ &\quad -(1118.34 - 491.85) \\ &= -2.41 \text{ eV}.\end{aligned}$$

The conduction band offset (ΔE_C) is

$$\Delta E_C = E_g^{FTO} - E_g^{GAO} - \Delta E_V, \quad (2)$$

i.e.,

$$\Delta E_C = 4.0 - 4.75 - (-2.41) = 1.66 \text{ eV}.$$

The energy differences between core energy levels and VBMs of Ga_2O_3 and FTO are expressed by $(E_{core} - E_{VBM})_{GAO}$ and $(E_{core} - E_{VBM})_{FTO}$, respectively. $(E_{core}^{GAO} - E_{core}^{FTO})_{GAO}^{FTO}$ is the binding energy difference for Ga $2p_{3/2}$ and Sn $3d_{3/2}$ core energies at the heterointerface between the Ga_2O_3 layer and FTO layer. In Eq. (2), E_g^{FTO} and E_g^{GAO} are the bandgaps for FTO (4.0 eV) and Ga_2O_3 (4.75 eV), as indicated in Refs. [22,24] and Fig. 1. Equations (1) and (2) allow us to determine the ΔE_V and ΔE_C, respectively. Table 1 is a summary of these values.

Figure 3(a) shows the diagram of the energy band alignment of the Ga_2O_3/FTO heterojunction. The ΔE_V of the heterojunction is -2.41 ± 0.02 eV and ΔE_C is 1.66 ± 0.02 eV in the operating hetero-structured devices,[25–27] allowed with deviations from measurement and calculation. Figure 3(a) suggests a staggered type-II energy band alignment of the Ga_2O_3/FTO heterojunction. The staggered type-II Ga_2O_3/FTO heterojunction misses the hole confinement.[10] The valence band offset and the conduction band offset are both greater than 1 eV, suggesting a large enough band offset for the successful fabrication of the heterojunction with rectification properties.[28] The obtained band offsets of the Ga_2O_3/FTO heterojunction are helpful for theoretical correction. Furthermore, it is worth noting that the heterojunction prepared here, unlike the high-temperature deposited heterojunction, does not have dense bonding, and may have space charge and/or an air insulating layer across the heterogeneous interface.

To explore the volt–ampere characteristics of the Ga_2O_3/FTO heterojunction, indium (In) electrodes are mechanically transferred onto the surfaces of FTO and Ga_2O_3, respectively. Figures 4(a) and 4(b) show a schematic diagram and a photograph of the Ga_2O_3/FTO heterojunction. In Fig. 4(c), the linear scale *I*–*V* curves of the Ga_2O_3/FTO heterojunction in the dark and under 254 nm UV light illumination are shown. It can be seen that the Ga_2O_3/FTO heterojunction presents rectified behavior, due to the discrete conduction band edges along with the large ΔE_C of 1.66 eV, as displayed in Fig. 3(b). Moreover, compared with the dark conditions, the rectification characteristics are increased under the ultraviolet light illumination of 254 nm; during this step the photo-generated electron–hole pairs are excited, the electrons move to the conduction band, while the holes correspondingly appear at the valence band, leading to an enhanced *I*–*V* performance under illumination. The log-scale *I*–*V* curves are presented in Fig. 4(d). The performance of the heterojunction is improved under 254 nm UV irradiation compared with that under dark conditions under conditions where the heterojunction interface is not treated by any physical or chemical techniques.

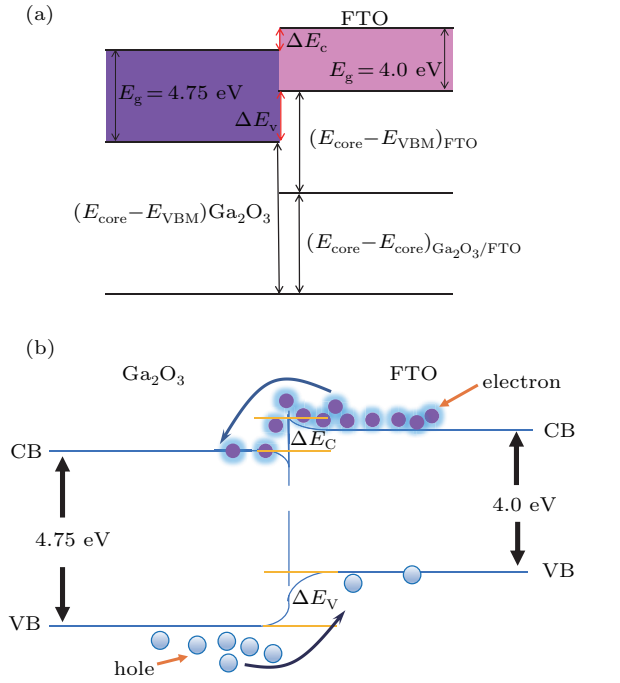


Fig. 3. The energy-band alignment diagram of the Ga_2O_3/FTO heterojunction.

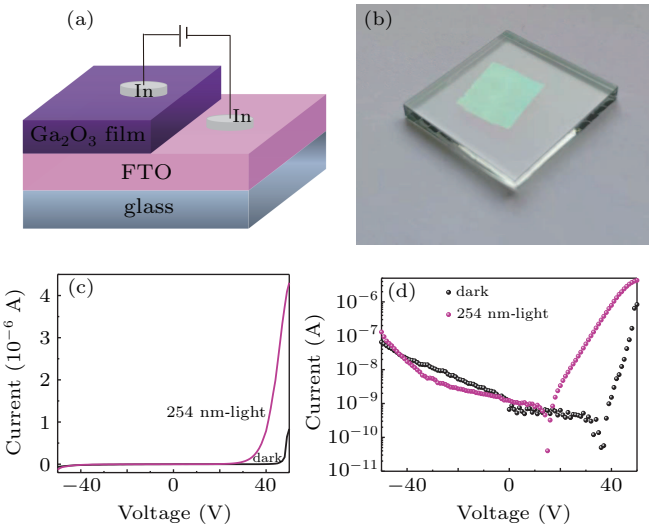


Fig. 4. The Ga_2O_3/FTO heterojunction on glass substrate: (a) a schematic diagram; (b) a photograph; (c) the linear scale *I*–*V* characteristics; and (d) the log-scale *I*–*V* characteristics.

In short, the work reported in this paper shows the feasibility of preparing a Ga_2O_3/FTO heterojunction. In addition, higher rectification performance of the Ga_2O_3/FTO heterojunction can be obtained using effective interior interface treatments and improved growth techniques. This is because the magnetron sputtering method always causes damage to the films, which may lead to metal contaminants and interfacial disorder.[29,30] Finally, in this work, the rectifying characteristics of the Ga_2O_3/FTO heterojunction were verified.

4. Conclusion

Based on Kraut's method, the band alignment of the Ga_2O_3/FTO heterojunction is studied using XPS in this paper. In particular, the Ga_2O_3/FTO heterojunction exhibits a staggered type-II band alignment accompanied with ΔE_C of 1.66 ± 0.02 eV and ΔE_V of -2.41 ± 0.02 eV. At the same time, the rectification ratio of the heterojunction was measured under the conditions of 254 nm light illumination and darkness. Based on the above results, some conclusions can be drawn from the Ga_2O_3/FTO heterojunction studied here with good rectifying behavior, and it is expected to be further applied to hetero-structured optoelectronic and electronic devices.

References

[1] Wilson A H 1939 *Semiconductors and Metals* (Cambridge: Cambridge University Press)
[2] Robertson J 2000 *J. Vac. Sci. Technol. B* **18** 1785
[3] Mannhart J and Schlom D 2010 *Science* **327** 1607
[4] Bayraktaroglu B 2017 *Assessment of Gallium Oxide Technology* (America: the USA 88th Air Base Wing) (88 ABW)
[5] Hwang W, Verma A, Peelaers H, Protasenko V, Rouvimov S, Xing H, Seabaugh A, Haensch W, Van de Walle C and Galazka Z 2014 *Appl. Phys. Lett.* **104** 203111
[6] Tsao Y, Chowdhury S and Hollis M 2018 *Adv. Electron. Mater.* **4** 1600501
[7] Liu Z, Li P, Zhi Y, Wang X, Chu X and Tang W 2019 *Chin. Phys. B* **28** 017105
[8] Rao C, Fei Z, Che, W, Chen Z, Lu X, Wang G, Wang X, Liang J and Pei Y 2020 *Chin. Phys. B* **29** 097303
[9] Zhi Y, Liu Z, Wang X, Li S, Wang X, Chu X, Li P, Guo D, Wu Z and Tang W 2020 *J. Vac. Sci. Technol. A.* **38** 023202
[10] Liu Z, Liu Y, Wang X, Li W, Zhi Y, Wang X, Li P and Tang W 2019 *J. Appl. Phys.* **126** 045707
[11] Tersoff J 1984 *Phys. Rev. B* **30** 4874
[12] Baik K H, Bevlin K, Carey I V P H, *et al.* 2019 *Gallium Oxide: Technology, Devices and Applications* (Amsterdam: Elsevier)
[13] Zhu B, Liu F, Li K, Lv K, Wu J, Gan Z, Liu J, Zeng D and Xie C 2017 *Ceram. Int.* **43** 10288
[14] Chen C, Lee W, Chen Y, Lu C, Lin H and Wu C 2015 *Adv. Mater.* **27** 4883
[15] Zhang J, Lou Y, Liu M, Zhou H, Zhao Y, Wang Z, Shi L, Li D and Yuan S 2018 *ACS Appl. Mater. Interfaces* **10** 15697
[16] Afre R, Sharma N, Sharon M and Sharon M 2018 *Review On Advanced Materials Science* **53** 79
[17] Li Z, Xu Y, Zhang J, Cheng Y, Chen D, Feng Q and Xu S 2019 *IEEE Photon. J.* **11** 6803709
[18] Sun H, Castanedo C, Liu K, Li K, Guo W, Lin R, Liu X, Li J and Li X 2017 *Appl. Phys. Lett.* **111** 162105
[19] Mastro M, Kuramata A, Calkins J, Kim J, Ren F and Peartong S 2017 *ECS J. Solid State Sci. Technol.* **6** P356
[20] Kraut E, Grant A, Waldrop J and Kowalczyk S 1980 *Phys. Rev. Lett.* **44** 1620
[21] Waldrop J, Grant R, Kowalczyk S and Kraut E 1985 *J. Vac. Sci. Technol. A* **3** 835
[22] Wang X, Wu Z, Cui W, Zhi Y, Li Z, Li P, Guo D and Tang W 2019 *Chin. Phys. B* **28** 017305
[23] Wang X, Chen Z, Guo D, Zhang X, Wu Z, Li P and Tang W 2018 *Opt. Mater. Express* **8** 2918
[24] Ikhmayies S 2016 *International Journal of Hydrogen Energy* **41** 12626
[25] Faber H, Das S, Lin Y, Pliatsikas N, Zhao K, Kehagias T, Dimitrakopulos G, Amassian A, Patsalas P and Anthopoulos T 2017 *Sci. Adv.* **3** e1602640
[26] Klein A 2012 *Thin Solid Films* **520** 3721
[27] Van de Walle C and Neugebauer J 2003 *Nature* **423** 62
[28] Xie C, Lu X, Tong X, Zhang Z, Liang F, Liang L, Luo L and Wu Y 2019 *Adv. Funct. Mater.* **29** 1806006
[29] Liu Z, Wang X, Zhi Y, Wang X, Chu X, Li S, Yan Z, Li P and Tang W 2019 *Phys. Status Solidi A* **216** 1900570
[30] Klein A 2015 *J. Phys. Condens. Matter* **27** 134201